INTERNATIONAL ATOMIC ENERGY AGENCY
UNITED NATIONS EDUCATIONAL, SCIENTIFIC AND CULTURAL ORGANIZATION
INTERNATIONAL CENTRE FOR THEORETICAL PHYSICS
I.C.T.P., P.O. BOX 586, 34100 TRIESTE, ITALY, CABLE: CENTRATOM TRIESTE

SMR.853 - 26

ANTONIO BORSELLINO COLLEGE ON NEUROPHYSICS

(15 May - 9 June 1995)

"Dynamic synaptic modification threshold: Computational model of experience-dependent plasticity in adult rat barrel cortex"

Mathew E. Diamond
Department of Sciences and Biomedical Technologies
Section of Physiology
University of Udine
33100 Udine
Italy

These are preliminary lecture notes, intended only for distribution to participants.

Proc. Natl. Acad. Sci. USA
Vol. 91, pp. 4791–4795, May 1994
Neurobiology

Dynamic synaptic modification threshold: Computational model of experience-dependent plasticity in adult rat barrel cortex

LUBICA BEŇUŠKOVÁ*, MATHEW E. DIAMOND, AND FORD F. EBNER†

Institute for Developmental Neuroscience, Vanderbilt University, Nashville, TN 37203

Communicated by Leon N Cooper, December 17, 1993 (received for review September 15, 1993)

ABSTRACT **Previous electrophysiological experiments have documented the response of neurons in the adult rat somatic sensory ("barrel") cortex to whisker movement after normal experience and after periods of experience with all but two whiskers trimmed close to the face (whisker "pairing"). To better understand how the barrel cortex adapts to changes in the flow of sensory activity, we have developed a computational model of a single representative barrel cell based on the Bienenstock, Cooper, and Munro (BCM) theory of synaptic plasticity. The hallmark of the BCM theory is the dynamic synaptic modification threshold, θ_M, which dictates whether a neuron's activity at any given instant will lead to strengthening or weakening of the synapses impinging on it. The threshold θ_M is proportional to the neuron's activity averaged over some recent past. Whisker pairing was simulated by setting input activities of the cell to the noise level, except for two inputs that represented untrimmed whiskers. Initially low levels of cell activity, resulting from whisker trimming, led to low values for θ_M. As certain synaptic weights potentiated, due to the activity of the paired inputs, the values of θ_M increased and after some time their mean reached an asymptotic value. This saturation of θ_M led to the depression of some inputs that were originally potentiated. The changes in cell response generated by the model replicated those observed in *in vivo* experiments. Previously, the BCM theory has explained salient features of developmental experience-dependent plasticity in kitten visual cortex. Our results suggest that the idea of a dynamic synaptic modification threshold, θ_M, is general enough to explain plasticity in different species, in different sensory systems, and at different stages of brain maturity.**

Although some forms of experience-dependent cortical plasticity disappear at the end of a developmental "critical" period (1, 2), the adult cortex retains a significant capacity to undergo functional changes in response to alterations in sensory input (3, 4). We are interested in the rules that determine how the adult rat whisker system adapts to changes in the pattern of afferent activity. The facial whiskers of rats are aligned in five rows (row A is dorsal and row E is ventral) and the whiskers within a row are numbered from caudal to rostral. Each facial whisker projects via the trigeminal nuclei and the thalamic ventral posterior medial nucleus (VPM) to a separate cluster of neurons in layer IV of a cortical barrel (5–8). Recently, we observed that the receptive fields (RFs) of neurons in adult rat barrel cortex were changed by altered whisker use (refs. 9–11; M.E.D., L.B., M. A. Nicolelis, F.F.E., and J. K. Chapin, unpublished work). To alter the pattern of sensory activity, all whiskers except two, D2 and one neighbor in the D row, were cut close to the fur on one side of the face. After 3, 7–10, or 30 days of whisker pairing (whiskers were reclipped regularly), the activity of single neurons in barrel D2 was measured in response to controlled deflection of the two paired whiskers, D2 and "D-paired," and the three cut neighbors (D-cut, C2, and E2). A progressive and complex modification of barrel D2 cell responses during the course of paired whisker experience was documented. The physiological study outlined above motivated us to develop a computational model of a barrel D2 neuron. The weights of the synaptic inputs to the modeled neuron are modifiable according to the Bienenstock, Cooper, and Munro (BCM) theory (12). This theory postulates that the neuron possesses a synaptic modification threshold, θ_M, that changes as a nonlinear function of the time-averaged postsynaptic activity. In the present simulation, due to the potentiation of the paired inputs' weights, the initially small mean value of θ_M gradually increases by about 50% before reaching an asymptote. This evolution of θ_M leads to changes in the computed efficacy of excitatory synapses impinging on the barrel D2 cell, and the changes in cell response match the empirical electrophysiological observations. The ability of the present and previous BCM models (13, 14) to explain complex experimental findings argues that the θ_M reflects an actual physiological mechanism.

MODEL AND RESULTS

Physiological and Anatomical Basis of the Barrel Cortex Circuit. According to studies in urethane-anesthetized rats, the RF of a cell in barrel D2 consists of two distinct components, a strong input from one whisker (the center RF, CRF) and a weaker input from several surrounding whiskers (surround RF, SRF). When the CRF whisker D2 is deflected, cells in barrel D2 yield nearly 50 spikes in 50 trials (10, 15). Of this total, about 30% occur at a short poststimulus latency (0–10 ms) and the remainder at a long poststimulus latency (10–100 ms). Short-latency spikes are evoked by a direct pathway from VPM. Long-latency spikes, in contrast, depend mainly on short intracortical circuits within barrel column D2 (16–18). When one of the SRF whiskers (D1, D3, C2, or E2) is stimulated, cells in barrel D2 yield about 15 spikes in 50 trials (10). Of these spikes, only a few occur at a short poststimulus latency (0–10 ms); >95% occur at a long latency (10–100 ms). The SRF is mediated mainly by horizontal intracortical pathways from neighboring barrels (16–19). Fig. 1 summarizes the excitatory inputs converging on a representative cell in barrel D2, and this is the simple circuit we use to model barrel cortex.

Experimental Observations of Barrel Cortex Plasticity. In electrophysiological experiments (refs. 9–11; M.E.D., L.B., M. A. Nicolelis, F.F.E., and J. K. Chapin, unpublished work), whisker D2 and one neighbor, D-paired (D1 or D3), were left intact while all other whiskers were cut. The observed plasticity in no way depended on whether D-paired

The publication costs of this article were defrayed in part by page charge payment. This article must therefore be hereby marked "*advertisement*" in accordance with 18 U.S.C. §1734 solely to indicate this fact.

Abbreviations: RF, receptive field; CRF, center RF; SRF, surround RF; VPM, ventral posterior medial nucleus; BCM, Bienenstock, Cooper, and Munro.

*On leave of absence from Neurophysics Group, Institute of Animal Biochemistry and Genetics, Slovak Academy of Sciences, 90028 Ivanka pri Dunaji, Slovakia.
†To whom reprint requests should be addressed.

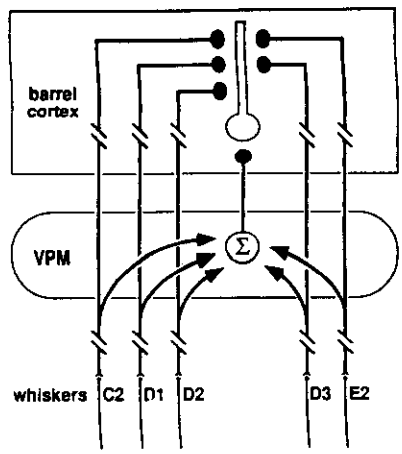

FIG. 1. Barrel cortex circuit used in the model. Whiskers C2, D1, D2, D3, and E2 converge through polysynaptic pathways (broken lines) upon a cell in VPM barreloid D2. The summation sign in the VPM barreloid denotes the multiwhisker character of the VPM cell. The synaptic inputs that are modifiable in our model are denoted by the filled circles in barrel cortex. At the present stage of the model we do not consider modifiability of the subcortical synapses (denoted by arrows) or other polysynaptic pathways (broken lines), although we do not exclude these possibilities.

was D1 or D3. The short-latency response (VPM-to-layer IV input) and long-latency response (intracortical inputs) of barrel D2 cells were tested after 3, 7–10, or 30 days of whisker pairing (Fig. 2). A monotonic increase in the number of short-latency spikes evoked both by whisker D2 and by whisker D-paired was observed. In addition, the number of short-latency spikes evoked by cut whiskers also increased. The plasticity of the long-latency (intracortical) inputs was characterized by a different time course. The long-latency response evoked by all cut whiskers decreased monotonically as the period of whisker pairing increased. On the other hand, long-latency activity evoked by both intact whiskers, D2 and D-paired, exhibited a curious inverted-U function, as follows. Initially, the number of long-latency spikes increased nearly 100% above control values. After 30 days of whisker pairing, however, D2 and D-paired evoked approximately the same number of long-latency spikes as in control cases.

Synaptic Modification in the BCM Theory. According to the BCM theory (12, 20), in the case of a linear cell, the modification of the ith synapse with the weight m_i at time t is proportional to the product of input activity at the ith synapse, $d_i(t)$, and a function ϕ, in such a way that

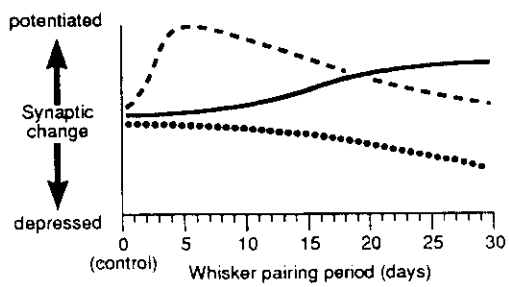

FIG. 2. Summary of the electrophysiological findings of barrel D2 cell plasticity produced by whisker pairing. Three types of cortical plasticity were observed: (*i*) monotonic potentiation of short-latency (0–10 ms poststimulus) responses to all whiskers, paired and cut (solid line); (*ii*) initial potentiation (up to ≈5 days), followed by gradual weakening (5–30 days) of the long-latency (10–100 ms poststimulus) responses to whiskers D2 and D-paired (dashed line); and (*iii*) monotonic weakening of the long-latency responses to all cut whiskers (dotted line).

$$\frac{dm_i(t)}{dt} = \eta\phi[c(t), \theta_M(t)]d_i(t). \quad [1]$$

The "modification rate," $\eta > 0$, is equal to the magnitude of the synaptic modification for the ith input in one time step, when $\phi = 1$ and $d_i = 1$. According to Intrator and Cooper (20), ϕ is a parabolic function of the cell's current firing rate $c(t)$ and modification threshold $\theta_M(t)$—i.e., $\phi[c(t), \theta_M(t)] = c(t)[c(t) - \theta_M(t)]$. Firing rate is in turn linearly proportional to the weighted sum of incoming activity, so that $c(t) = \Sigma m_i(t)d_i(t)$. The dynamic modification threshold $\theta_M(t)$ is a nonlinear function of the time-averaged postsynaptic activity $c(t)$, so that

$$\theta_M(t) = \left[\frac{\langle c^2(t)\rangle_\tau}{c_0}\right], \quad [2]$$

where c_0 is a positive scaling constant. The averaged cell activity over some recent past $\langle c^2(t)\rangle_\tau$ is determined by the following integral:

$$\langle c^2(t)\rangle_\tau = \frac{1}{\tau}\int_{-\infty}^{t} c^2(t')e^{-\left[\frac{(t-t')}{\tau}\right]}dt', \quad [3]$$

where τ is the averaging period. From these relations it follows that when postsynaptic activity $c(t)$ is greater than zero but less than the modification threshold θ_M, all active synapses [i.e., $d_i(t) > 0$] weaken. On the other hand, when postsynaptic activity $c(t)$ is greater than θ_M, all active synapses potentiate. Since $c(t) = \Sigma m_i(t)d_i(t)$, the correlation (synchronicity, pairing) of excitatory inputs plays a crucial role in driving the postsynaptic cell activity above the modification threshold θ_M. The key property of θ_M is that it is not fixed; instead, its current value is proportional to the postsynaptic response averaged over some recent past time.

Barrel D2 Model Neuron. Each whisker influences the barrel D2 cell through both thalamocortical and corticocortical circuits (Fig. 1), but the input strengths (I values) of these components for the various whiskers differ. The overall VPM input at given time instant t, $d^{VPM}(t)$, consists of the sum of activities, $d_j^{VPM}(t)$, evoked in the VPM barreloid D2 by deflections of combinations of five whiskers—e.g.,

$$d^{VPM}(t) = \sum_{j=1}^{5} d_j^{VPM}(t) = \sum_{j=1}^{5}[I_j^{VPM}d(t) + n_j^{VPM}(t)]. \quad [4]$$

In parallel with the activity of intracortical input $d_j^{cor}(t)$ associated with the deflection of the jth whisker is equal to

$$d_j^{cor}(t) = I_j^{cor}d(t) + n_j^{cor}(t). \quad [5]$$

In these equations, $d(t)$ is equal to either 1 or 0, depending on whether or not the jth whisker is deflected. $0 < I_j^{VPM} < 1$ and $0 < I_j^{cor} < 1$ are the input strength constants of the jth whisker input conveyed through the barreloid D2 and intracortical synapses, respectively. The noise, either $n_j^{cor}(t)$ or $n_j^{VPM}(t)$, is defined as a random variable uniformly distributed in the interval $[-A(\text{noise}), +A(\text{noise})]$, where A is the noise amplitude. The noise reflects the stochastic fluctuations in the corresponding input activity.

The value of $c(t)$ is obtained by multiplying the activity $d_i(t)$ of each input by its corresponding synaptic weight $m_i(t)$ and summing over all synaptic inputs to the cell; i.e.,

$$c(t) = \sum_{i=1}^{6} m_i(t)d_i(t) = m^{VPM}(t)d^{VPM}(t) + \sum_{j=1}^{5} m_j^{cor}(t),d_j^{cor}(t), \quad [6]$$

2.

where $m_i(t)$ modifies according to Eq. 1. The first term in Eq. 6 represents the short-latency response component and the second term represents the long-latency response. As suggested by Fig. 1 and Eqs. 4–6, each of the five intracortical inputs has its own modifiable input weight $m_j^{cor}(t)$, but the multiwhisker input from the VPM barreloid D2 is represented by one modifiable weight, $m^{VPM}(t)$.

Computer Simulation of Whisker Pairing. At each time step, a pattern of activity $d(t) = \{d_i(t)\}$ was generated that represents the activity of the inputs corresponding to the five whiskers D2, D1, D3, C2, and E2. To simulate clipping the whiskers, the input activities for j = D-cut, C2, and E2 were set to the noise for 100% of time steps—e.g., $d_j^{VPM}(t) = n_j^{VPM}(t)$ and $d_j^{cor}(t) = n_j^{cor}(t)$ (see Eqs. 4 and 5). The two paired whiskers D2 and D-paired "produced" noise (i.e., were unstimulated) 84% of the time. During this time, $d_j^{VPM}(t) = n_j^{VPM}(t)$ and $d_j^{cor}(t) = n_j^{cor}(t)$ for j = D2, D-paired. The remaining 16% of total time was divided among three possible combinations of deflection of the two whiskers, i.e., {1, 1}, {1, 0}, and {0, 1}, with the percent time 22%, 39%, and 39%, respectively. Here the first combination represents synchronous deflection of the whiskers and the two latter combinations represent their asynchronous deflections. The significance and range of the percent time devoted to the deflections of the two spared whiskers, as well as the percent time divided between the synchronous and asynchronous deflections, will be discussed later. In this subsection we present the values of parameters with which we obtained the best quantitative agreement between the simulated and experimental results.

The crucial factor in modeling the input to the barrel D2 cell is the input strength constant of different whisker inputs conveyed from VPM ($0 < I_j^{VPM} < 1$) and from intracortical sources ($0 < I_j^{cor} < 1$). The values and ratios I_j^{VPM}/I_j^{cor} that led to satisfactory simulation of the whisker pairing condition were 0.75/0.85 for D2, 0.05/0.95 for D1, 0.025/0.975 for D3, and 0.05/0.95 for C2 and E2.

Once the vector $d(t)$ was constructed, the resulting cell response $c(t)$ was calculated according to Eq. 6, and the changes in synaptic weights $dm_i(t)/dt$ were determined according to Eq. 1. The component values of the weight vector $m(0) = \{m^{VPM}(0), m_1^{cor}(0), \ldots, m_5^{cor}(0)\}$, with which we started the simulation of whisker pairing, were calculated such that the short- and long-latency responses of the barrel D2 cell would be equal to the experimental control values. Thus, the value of $m^{VPM}(0)$ was calculated from the set of equations for short-latency responses—e.g., $c_j = m^{VPM}(0)I_j^{VPM}$, for j = D2, D1, D3, C2, and E2. The values of $m_j^{cor}(0)$ were calculated according to the equations for the long-latency responses—e.g., $c_j = 9.0m_j^{cor}(0)I_j^{cor}$, for j = D2, D1, D3, C2, and E2. In this calculation we took into account the fact that the long-latency response is the sum of barrel D2 discharges over the time interval 10–100 ms, which is 9 times greater than the time interval over which the short-latency response is counted. The calculated initial weights values were: $\{m^{VPM}(0), m_1^{cor}(0), \ldots, m_5^{cor}(0)\} = \{0.43, 0.1, 0.08, 0.049, 0.045, 0.045\}$.

For updating the weights, at each time step the average cell activity over the recent past and the value of θ_M need to be calculated. The chosen values for the averaging period (Eq. 3), scaling constant (Eq. 2), and modification rate (Eq. 1) were $\tau = 10$, $c_0 = 0.12$, and $\eta = 0.0001$, respectively.

The relation between the number of computer iterations and real time was established as follows: since extrapolation of empirical data indicates that the maximal responses to whisker D2 and D-paired occur after about 5 days of pairing, and the simulated peaks occur around 500,000 iterations, each day of whisker pairing was equated with 100,000 iterations.

At regular intervals the model cell was "tested" by calculation of the short-latency and long-latency responses evoked by individual "deflection" of each of the five whiskers. The results of computer simulations of the whisker pairing are illustrated in Fig. 3. The changes in short-latency and long-latency responses of the barrel D2 model cell qualitatively and quantitatively parallel those observed in experiment (refs. 9–11; M.E.D., L.B., M. A. Nicolelis, F.F.E., and J. K. Chapin, unpublished work).

Dynamics of the Synaptic Modification Threshold θ_M. For illustration of the overall evolution of θ_M, we calculated the mean value of θ_M for each simulated day (Fig. 4). Setting all except two inputs to noise results in a relatively small average cell activity. Since θ_M is proportional to the square of the cell's activity averaged over a recent past (Eq. 2), the values of θ_M and consequently the illustrated mean value of θ_M are

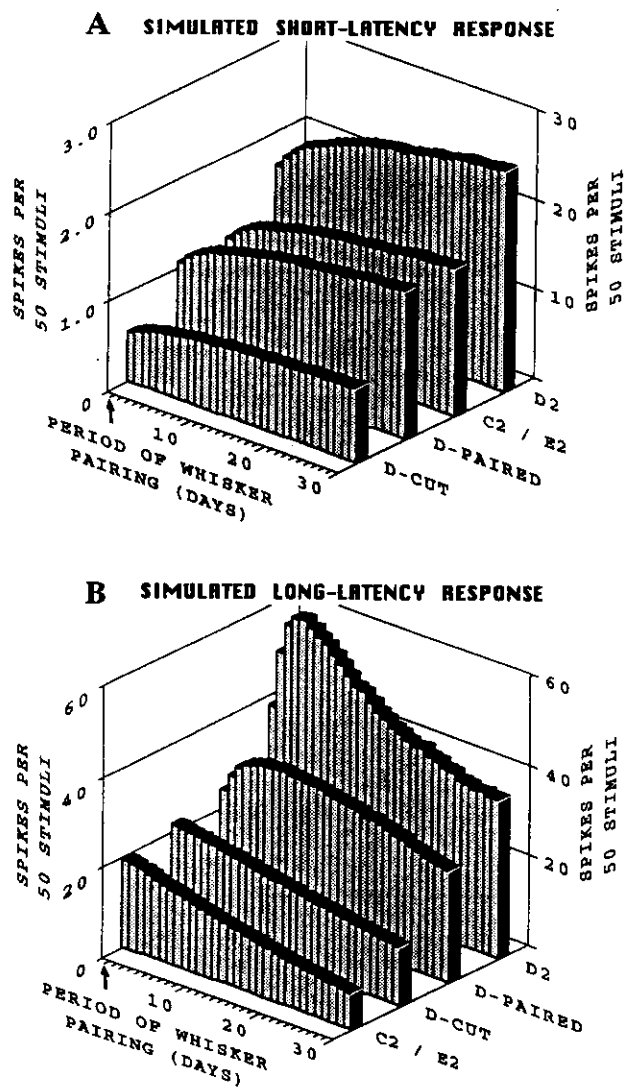

FIG. 3. Simulation of barrel D2 cell responses during 30 days of whisker pairing. Arrow indicates onset of whisker pairing. The evolution of short-latency and long-latency cell responses parallels that observed experimentally; compare with Fig. 2. Here, the D-paired plots start from the control values for whisker D1, and the D-cut plots start from the control values for D3. However, reversing the two starting points did not affect the qualitative and quantitative evolution of simulated responses. (*A*) Short-latency responses in the poststimulus interval 0–10 ms. Note that the left axis applies to response values for SRF whiskers and the right axis applies to values for whisker D2. (*B*) Long-latency responses in the poststimulus interval 10–100 ms.

3.

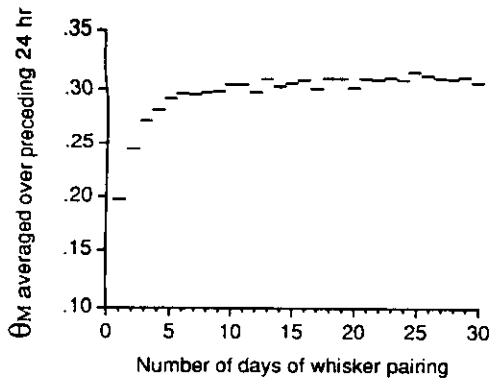

FIG. 4. Evolution of the synaptic modification threshold θ_M during whisker pairing. See text for description.

smallest for the first simulated day. Then, due to gradual potentiation of the short-latency (VPM) input and two long-latency (intracortical) inputs from the paired whiskers, the average postsynaptic activity, $\langle c^2(t)\rangle_\tau$, increases. Proportional to $\langle c^2(t)\rangle_\tau$, the values of θ_M increase, so that by about the fifth simulated day their mean reaches its asymptotic value. Around this point the long-latency inputs from paired whiskers start to weaken, since they evoke activity that falls below current θ_M most of the time (see *Discussion*). The tendency of the potentiating short-latency input to increase cell activity and the tendency of the weakening long-latency inputs to decrease cell activity are in competition; a dynamic balance is created that causes the mean value of θ_M to oscillate around its asymptotic value.

DISCUSSION

Summary. By computer simulation, we have shown that the BCM model of a single representative cell in barrel D2 successfully reproduces the three types of plasticity observed *in vivo* in whisker pairing experiments (refs. 9–11; M.E.D., L.B., M. A. Nicolelis, F.F.E., and J. K. Chapin, unpublished work): (*i*) monotonic increase in the short-latency (0–10 ms) responses to all whiskers, (*ii*) monotonic decrease in the long-latency (10–100 ms) responses to all cut whiskers, (*iii*) initial increase in the long-latency responses to the paired whiskers, D2 and its spared D-row neighbor (D1 or D3), followed by a decrease in these responses. Consistent with the known physiology and anatomy of the barrel cortex (Fig. 1), short-latency responses are evoked through a multiwhisker channel interpreted as the input from VPM barreloid D2. The long-latency SRF inputs are mediated by single-whisker inputs interpreted as polysynaptic pathways from neighboring barrel columns. The long-latency input from the CRF, whisker D2, is interpreted as a polysynaptic connection within barrel column D2.

Sensitivity of the Model to the Values of Parameters. In our simulations, the modification rate $0.0 < \eta \leq 0.001$ determined the speed of synaptic weight changes but did not determine their sign and magnitude. The values of $\eta > 0.001$ led to oscillations of the modeled cell response. In contrast, the sign, magnitude, and time course of synaptic weight changes depended on the number of iterations $10 \leq \tau \leq 10^4$ over which cell activity was averaged in the calculation of θ_M (Eq. 3). Large values of τ mean that the neuron had a long "memory" of past activity. Values of $\tau > 10^4$ led to oscillations of the modeled cell response. On the other hand, very short memory of the past activity, represented by the values $\tau < 10$, resulted in monotonic depression of all the inputs. For the given range of η, the range of τ corresponded to $\approx$1 s to $\approx$140 min of real time. For comparison, τ used in modeling visual cortex developmental plasticity was equated to 22 min (13). If for $\eta = 10^{-4}$ the value of $\tau = 1.4 \times 10^3$, which corresponds to 20 min, all the responses of the model barrel D2 cell departed quantitatively from the experimental values, by up to 100%, but the qualitative evolution was preserved. In general, when τ was large (on the order of minutes) the value of modification rate η had to be small in order to prevent oscillations in the cell's response. To produce the best quantitative agreement with the experimental data (Fig. 3), the averaging period τ in our simulations was on the order of seconds.

The input strength constants for CRF and SRF inputs conveyed through VPM and through intracortical connections had a prominent influence on the sign, magnitude, and time course of synaptic weight changes. We used the values of $0 < I_j^{VPM} < 1$ and $0 < I_j^{cor} < 1$. These constants were introduced to reflect different magnitudes of the control short- and long-latency responses of the barrel D2 cell to the stimulation of the CRF and SRF whiskers. Qualitative and quantitative agreements with experimental data were obtained when the input strength constant associated with the VPM synapse is much greater for D2 than for the other whiskers—i.e., $I_{D2}^{VPM} >> I_j^{VPM}$ for j = D1, D3, C2, and E2. For the SRF whiskers the input strength constants associated with intracortical circuits must be much larger than that conveyed by VPM—i.e., $I_j^{cor} >> I_j^{VPM}$ for j = D1, D3, C2, and E2. When the latter two ratios are reversed the experimental data cannot be replicated either quantitatively or qualitatively. For the CRF whisker, the cortical input strength constant must be equal to or a little greater than the VPM input strength constant—i.e., $I_{D2}^{cor} \geq I_{D2}^{VPM}$, for the quantitative agreement. The last ratio can be arbitrary for qualitative reproduction of the experimental data. All above ratios between VPM and cortical input strength constants are in accordance with what is known about the construction of CRFs and SRFs in barrels (refs. 15–19; also compare the control short- and long-latency responses for CRF and SRF whiskers in Fig. 3).

Similarly, the fractions of time divided between various combinations of whisker deflection (synchronous vs. asynchronous), and the total amount of time during which the two whiskers are deflected, have a profound effect on the course of synaptic plasticity. The qualitative (and quantitative) agreement with experimental data can be obtained whenever the percent time during which the two spared whiskers are deflected is in the interval 13–23%. According to available data (21), the duration of a rat's activity time depends on many variables—e.g., duration of light, light intensity, period of the light–dark cycle, social cues, and hormone cycles. However, we did not measure this time in our experimental animals. Since this variable can be easily manipulated, it may serve as a mean for further testing of the model. In our simulations, when the two whiskers were deflected for a total amount of time greater than 23%, the long-latency response to D-paired monotonically potentiated.

Insights into Barrel Cortex Plasticity Resulting from the BCM Model. The key to the successful simulation of the three types of experience-evoked plasticity is the behavior of the synaptic modification threshold, θ_M (Fig. 4). Active excitatory synapses potentiate whenever the postsynaptic activity c is greater than θ_M; active synapses weaken when c is less than θ_M. During tactile exploration, three combinations of the two spared whiskers' deflections are considered: both whiskers are bent synchronously during the contact with objects or asynchronously in one of the two possible sequences. The initial small value of θ_M allows short- and long-latency inputs conveying activity from the paired whiskers to evoke postsynaptic activity greater than θ_M, for all combinations of their deflections. Therefore, both short- and long-latency inputs belonging to the paired whiskers potentiate (Fig. 3). On the other hand, postsynaptic activity evoked by the random weak activity (the "noise") of inputs from cut whiskers falls below

4.

even the small value of θ_M. This causes long-latency inputs associated with all the cut whiskers to weaken. Noise associated with the cut whiskers also tends to weaken the multiwhisker short-latency VPM input. However, activity from the paired whiskers, D2 and D-paired, tends to strengthen VPM input. Due to a strong D2 activity component, the balance between the strengthening and weakening of the VPM input is shifted in favor of its strengthening. The potentiation of the VPM synapse allows increased short-latency input from all whiskers, including the cut ones, since all whiskers have a common short-latency input to the cortical cell through VPM. When θ_M approaches its asymptotic value (due to an increase in average cell activity), individual deflections of the two spared whiskers are no longer able to drive the barrel D2 cell activity above θ_M. Subsequent gradual depression of the long-latency inputs from the paired whiskers results from the fact that in the simulations sequential asynchronous deflections of whiskers are more frequent than simultaneous deflections. Asynchronous activity is insufficient to drive the postsynaptic cell activity above θ_M, with the result that the strengths of long-latency inputs decrease (Fig. 5). This tends to cause a decrease in the average cell activity and in the value of θ_M. Due to this tendency, the strong short-latency VPM input can continue to potentiate. In turn, this potentiation tends to increase the average cell activity and the value of θ_M, so that the strength of long-latency inputs continues to decrease. The tendency of the weakening long-latency inputs to decrease the cell activity and tendency of the potentiating short-latency input to increase cell activity are in competition; a dynamic balance is created that causes θ_M and consequently its mean value to oscillate around the asymptotic value (Fig. 4).

On the Physiological Mechanism of θ_M. On the basis of experimental findings on visual cortex plasticity, it has been proposed (22) that θ_M may represent the membrane potential at which the Mg^{2+} block of *N*-methyl-D-aspartate receptor-gated ion channels is removed, allowing postsynaptic Ca^{2+} entry. Increased Ca^{2+} influx would result in enhanced synaptic efficacy through a number of mechanisms (23), whereas activated synapses accompanied by weak or no postsynaptic

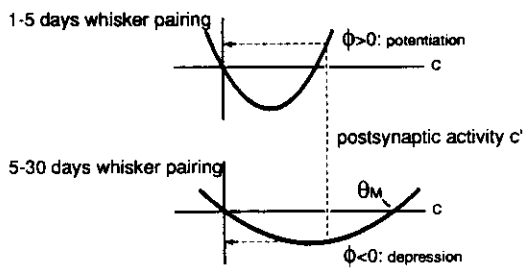

FIG. 5. Schematic illustration of how the same level of postsynaptic activity c' can result in synapse potentiation or depression depending on the current value of the synaptic modification threshold θ_M. According to the BCM synaptic modification rule, active inputs $d_i > 0$ are strengthened when postsynaptic activity $c > \theta_M$ and $\phi > 0$. Active inputs weaken when $c < \theta_M$ and $\phi < 0$. In our simulation, the initial small value of θ_M (*Upper*) allows long-latency inputs conveying activity from the paired whiskers to evoke cell response greater than θ_M, for both synchronous and asynchronous combinations of their deflections. Postsynaptic activity evoked by asynchronous deflections is denoted as c'. When θ_M approaches its asymptotic value (*Lower*), asynchronous deflections of the two spared whiskers producing the same level of cell activity c' are no longer able to drive the barrel D2 cell above θ_M. When asynchronous deflections are more frequent than synchronous deflections, the net effect is a weakening of the long-latency inputs from the paired whiskers.

Ca^{2+} would be weakened over time. This hypothesis can be applied to the barrel neurons, too, since it has been shown that most of the whisker-evoked activity in adult rat barrel cortex is dependent upon *N*-methyl-D-aspartate receptor action (18). From the theoretical definition of θ_M it follows that the membrane potential at which Mg^{2+} block is removed should vary as a function of the history of prior cell activity. It is known that protein kinase C can modulate the voltage-dependency of Mg^{2+} block of the *N*-methyl-D-aspartate receptor-gated channel (24). The activity of protein kinase C can itself be modulated by the action of glutamate on its metabotropic receptors, by the action of acetylcholine, and by other transmitters such as opioids. Thus, protein kinase C could mediate the dependence of Mg^{2+} block on the previous history of cell activity. The ability of the BCM theory to explain a wide range of cortical plasticity phenomena should stimulate a concentrated search for the physiological mechanism of the dynamic synaptic modification threshold.

We express our appreciation to the members of the Institute for Brain and Neural Systems at Brown University for their hospitality and many useful conversations that helped to define the model—in particular, to Leon N Cooper, Nathan Intrator, Charlie Law, Michael P. Perrone, and Harel Z. Shouval. Our thanks go also to Michael Armstrong-James for his participation in discussions about barrel cortex physiology and anatomy.

1. Olson, C. R. & Freeman, R. D. (1980) *Exp. Brain Res.* **39**, 17–21.
2. Blakemore, C. & van Sluyters, R. C. (1974) *Br. J. Ophthalmol.* **58**, 176–182.
3. Clark, S. A., Allard, T., Jenkins, W. M. & Merzenich, M. M. (1988) *Nature (London)* **332**, 444–445.
4. Jenkins, W. M., Merzenich, M. M., Ochs, M. T., Allard, T. & Guíc-Robles, E. (1990) *J. Neurophysiol.* **63**, 82–104.
5. Woolsey, T. A. & Van der Loos, H. (1970) *Brain Res.* **17**, 205–242.
6. Welker, C. (1971) *Brain Res.* **26**, 259–275.
7. Jensen, K. F. & Killackey, H. P. (1987) *J. Neurosci.* **7**, 3529–3543.
8. Killackey, H. P. (1973) *Brain Res.* **51**, 326–331.
9. Diamond, M. E. & Armstrong-James, M. (1992) *Concepts Neurosci.* **3**, 55–78.
10. Diamond, M. E., Armstrong-James, M. & Ebner, F. F. (1993) *Proc. Natl. Acad. Sci. USA* **90**, 2082–2086.
11. Armstrong-James, M., Diamond, M. E. & Ebner, F. F. (1994) *J. Neurosci.*, in press.
12. Bienenstock, E. L., Cooper, L. N & Munro, P. W. (1982) *J. Neurosci.* **2**, 32–48.
13. Clothiaux, E. E., Bear, M. F. & Cooper, L. N (1991) *J. Neurophysiol.* **66**, 1785–1804.
14. Sklar, E. (1991) *Proceedings of the International Joint Conference on Neural Networks 1990*, Vol. 3, pp. 727–732.
15. Armstrong-James, M. & Fox, K. (1987) *J. Comp. Neurol.* **263**, 265–281.
16. Armstrong-James, M., Callahan, C. A. & Friedman, M. A. (1991) *J. Comp. Neurol.* **303**, 193–210.
17. Armstrong-James, M., Fox, K. & Das-Gupta, A. (1992) *J. Neurophysiol.* **68**, 1345–1358.
18. Armstrong-James, M., Welker, E. & Callahan, C. A. (1993) *J. Neurosci.* **13**, 2149–2160.
19. Armstrong-James, M. & Callahan, C. A. (1991) *J. Comp. Neurol.* **303**, 211–224.
20. Intrator, N. & Cooper, L. N (1992) *Neural Networks* **5**, 3–17.
21. Moore-Ede, M. C., Sulzman, F. M. & Fuller, C. A. (1982) *The Clocks That Time Us* (Harvard Univ. Press, Cambridge, MA).
22. Bear, M. F., Cooper, L. N & Ebner, F. F. (1987) *Science* **237**, 42–48.
23. Bliss, T. V. P. & Collingridge, G. L. (1993) *Nature (London)* **361**, 31–39.
24. Ben-Ari, Y., Aniksztejn, L. & Bregestovski, P. (1992) *Trends Neurosci.* **15**, 333–339.

5.